Gating current "fractionation" in crayfish giant axons

J. G. Starkus and M. D. Rayner*
Pacific Biomedical Research Center, Békésy Laboratory of Neurobiology; and the *Department of Physiology, John A. Burns School of Medicine, University of Hawaii, Honolulu, Hawaii 96822

ABSTRACT Effects of changes in initial conditions on the magnitude and kinetics of gating current and sodium current were studied in voltage-clamped, internally-perfused, crayfish giant axons. We examined the effects of changes in holding potential, inactivating prepulses, and recovery from inactivation in axons with intact fast inactivation. We also studied the effects of brief interpulse intervals in axons pretreated with chloramine-T for removal of fast inactivation.

We find marked effects of gating current kinetics induced by both prepulse inactivation and brief interpulse intervals. The apparent changes in gating current relaxation rates cannot be explained simply by changes in gating charge magnitude (charge immobilization) combined with "Cole-Moore-type" time shifts. Rather they appear to indicate selective suppression of kinetically-identifiable components within the control gating currents. Our results provide additional support for a model involving parallel, nonidentical, gating particles.

INTRODUCTION

The primary structure deduced for the *Electrophorus* sodium channel (Noda et al., 1984), indicated four pseudosymmetrical repeating regions within the α polypeptide chain. Several models have now been proposed for the folding of this chain across the membrane bilayer (Greenblatt et al., 1985; Numa and Noda, 1986; Guy and Seetharamulu, 1986). These models agree is suggesting that positively charged regions in each tetramer may function as voltage sensors for the channel molecule (perhaps in association with negatively charged surrounding structures; see Montal, 1990). A channel structure indicating four parallel voltage sensors has generated a return of interest in parallel kinetic models for voltage-regulated ion channels (Catterall, 1986; Zagotta and Aldrich, 1990; Keynes, 1990). However, the electrophysiological evidence has largely been opposed to the parallel Hodgkin-Huxley formulation (Hodgkin and Huxley, 1952b), favoring linear sequential models for the control of channel gating (see reviews by French and Horn, 1983; Armstrong and Matteson, 1984, and more recent studies such as Stimers et al., 1985, 1987).

On the other hand, substitution of deuterium oxide for water in the internal perfusate of voltage-clamped crayfish giant axons slows activation of sodium current without any corresponding change in deactivation rate or detectable effect on gating currents (Alicata et al., 1990). These observations confirmed the earlier findings of Schauf and Bullock (1979, 1980, 1982) and support their conclusion that solvent-insensitive deactivation cannot reflect mere reversal of the solvent-sensitive final activation step. The effects of deuterium oxide substitution are thus incompatible with linear sequential models for the channel activation mechanism. A more complex cyclic mechanism seems implicated, suggestive of multiple parallel gating mechanisms.

The earliest indications of parallel components within the gating currents were provided by Armstrong and Benzanilla (1974), who noted that gating currents are only partially immobilized by inactivating prepulses. That observation has been extensively confirmed for squid axons (Armstrong and Bezanilla, 1977; Greeff et al., 1982), frog myelinated nerve (Nonner, 1980), crayfish giant axons (Swensen, 1980; Starkus et al., 1981), *Myxicola* giant axons (Bullock and Schauf, 1980), and cardiac Purkinje cells (Hanck et al., 1989). In each case around one-third of total gating charge (Q_t) remains nonimmobilizable after inactivating prepulses of 20 to 30 ms duration. As Bekkers et al. (1984) pointed out: if the nonimmobilizable component (Q_n) is a nonspecific charge displacement unrelated to ion channel gating, why should the Q_n fraction be the same in both myelinated and nonmyelinated axons?

Greeff et al. (1982) compared the kinetics of control gating currents (Ig_t) and of the nonimmobilizable component (Ig_n) seen after an inactivating prepulse. Because Q_t is necessarily the sum of the nonimmobilizable Q_n and the immobilizable charge (Q_i), they estimated the time course of the immobilizable component of gating cur-

A part of this work has been presented in preliminary form (see Starkus and Rayner, 1987; Rayner and Starkus, 1991).

Address correspondence and reprint requests to Dr. John G. Starkus.

0006-3495/91/11/1101/19 $2.00

rent (Ig_i) by subtracting the observed Ig_n from the control Ig_t. This method for "fractionation" of the gating currents demonstrated considerably faster relaxation kinetics for Ig_n, as well as a faster time to peak for Ig_n (10 to 20 μs) than for Ig_i (50 to 100 μs). Subsequent pharmacological studies (Bekkers et al., 1984) showed that local anesthetics similarly immobilize only the Ig_i component, although both the Ig_n and Ig_i components were equally reduced by change of holding potential from −98 to −60 mV.

Fractionation of gating currents by this subtraction method may seem theoretically justifiable only if Ig_n and Ig_i are generated independently from parallel movements of noninteracting charges. There is additional evidence that might indicate a parallel origin for these major components of gating current. Keynes (1983) has argued that Ig_n must reflect a channel gate in parallel with the gate(s) controlled by Ig_i, because only the Ig_n component is fast enough to close sodium channels during the rapid deactivation seen on return to strongly negative holding potentials. Similarly, Bekkers et al. (1984) pointed out that Ig_n (identified by immobilizing prepulses) is the earliest component of gating current during both ON and OFF voltage steps. Again, a parallel origin for Ig_n seemed implicated.

By contrast, direct evidence suggestive of sequential processes in sodium channel gating was provided by Keynes and Rojas (1976) who demonstrated increasing delays in the rising phase of I_{Na} at more negative holding potentials. These "Cole-Moore-type" effects were further characterized by Hahin and Goldman (1978) using hyperpolarizing and depolarizing prepulses. Subsequently, quantitative equivalencies were reported between hyperpolarization-induced time delays in the rising phase of I_{Na} and the falling phase of IgON (Taylor and Bezanilla, 1983), as well as for the rising phases of I_{Na} and Ig_i (Keynes, 1986).

In this paper we reexamine the principal evidence for parallel origin of gating currents, using crayfish rather than squid giant axons. We confirm that charge immobilization associated with fast inactivation affects different kinetic components of gating current to differing extents. We also demonstrate, using short (~50 μs) prepulses, that the fastest gating current component behaves as a separate, parallel, gating particle. However, in crayfish axons, the subtraction method exposes a slow rising phase of "Ig_i" only within a restricted range of experimental conditions. Furthermore, fast inactivation can suppress peak gating current by as much as 40%, indicating that immobilizable charge movement rises together with the fast-relaxing nonimmobilizable component in crayfish axons. Thus, our work fails to confirm the separate identity of "Ig_i" suggested by the subtraction method. On the other hand, kinetic analysis of Ig_t and Ig_n records, together with Ig_i-type subtraction records, indicates that these difference currents can provide confirmatory evidence concerning the kinetic effects of changing initial conditions.

METHODS

Crayfish medial giant axons were dissected free, internally-perfused and voltage-clamped following methods initiated by Shrager (1974) and modified as described by Starkus et al. (1984) and Heggeness and Starkus (1986). Axons were maintained between 6° and 8°C; potassium currents were blocked by internal perfusion with solutions containing Cs or tetramethylammonium (TMA) ions (see below); sodium currents were blocked to permit recording of gating currents by adding 100 nM tetrodotoxin (TTX) to the external perfusate; fast inactivation was removed, when necessary, using chloramine-T (Sigma Chemical Co., St Louis, MO) following the procedure described by Alicata et al. (1990). Our pulse generation, data recording techniques, methods for subtraction of capacity currents, and both linear and nonlinear components of leakage current have been described by Rayner and Starkus (1989) and Alicata et al. (1989, 1990). Additional aspects of the methods used for this study are considered in more detail below.

Series resistance compensation

In this study, series resistance compensation was initially set to 10 ohm · cm² and then fine tuned (within the range 9 to 12 ohm · cm²) by comparing kinetics of sodium currents at 0 mV test potential, from holding potentials of −120 and −85 mV. Compensation was adjusted until we could detect no kinetic effects of the greater than twofold change in current magnitude produced by this shift in holding potential. Thereafter peak capacity current was monitored in voltage steps at very negative potentials (from −150 to 200 mV) and R_s adjustments were made as needed to maintain constant peak capacity current and hence constant clamp rise time (see Alicata et al., 1989).

Filtering

Early experiments in the sequence presented here were obtained using an adjustable Bessel filter set for cut-off at 500 kHz. All records were adjusted for the ~8-μs delay induced by this filter and then smoothed digitally according to the procedure described below. No analogue filtering was used for more recent experiments, although the digitization sampling interval effectively limits inputs at frequencies greater than 1 MHz (for 1-μs sample intervals) or 500 kHz (for 2-μs intervals). Data traces were recorded directly on hard disk. These traces were smoothed before analysis, using an adjustable smoothing routine applied according to the following criteria: for the first 50 μs after the start of a voltage step, no filtering; the next 50 μs was filtered at 100 khz; the next 100 μs, at 50 kHz; the remainder of the record, 10 kHz. Where multiple voltage steps were imposed during a single trace, this sequence was restarted for each voltage step. Overlay of smoothed and unfiltered traces showed no detectable time shifts or kinetic distortions introduced by this smoothing procedure.

Data analysis

Data traces for kinetic analysis were recorded at 1-μs sample intervals and filtered as described above. Kinetic analysis was carried out using the OLIS KINFIT programs (On-Line Instrument Systems, Inc., Jefferson, GA). The KINFIT programs permit choice of a modified Levenberg-Marquardt routine or a Successive Integration routine for

identification of up to four exponential components. In our data, time-constant separation appears adequate for three component analysis although noise becomes a problem in identification of the slow time-constant, particularly after pulse protocols which selectively suppress this kinetic component (see Results). In all cases, our analyses were carefully assessed by on-screen inspection of the "residuals" record (created by subtraction of the sum of fitted exponentials from the original data trace). Candidate analyses were rejected if visually detectable kinetic deviations were found in this residuals trace (i.e., the residual must appear "flat" within the limits of the noise present on the original filtered data trace).

Terminology

Because our gating currents are well described by the sum of three exponentials, we shall refer to these analytical components as "fast" (τ_f), "intermediate" (τ_m), and "slow" (τ_s) without intending to imply that the same reciprocal eigenvalue is necessarily being recognized in each analysis.

Computer simulations

Simulations were carried out using a Sun 3/60 computer (Sun Microsystems, El Segundo, CA). Our modeling program employs simple Euler integration to solve the array of simultaneous equations representing the allowed transitions within each particular model formulation. Cumulative errors were less than 0.001% at the end of each model run. All voltage steps were presumed to be instantaneous. Holding potential was set to −120 mV for each simulation and calculated initial state occupancies were used for each model run. Multistep protocols were simulated using the final state occupancies from the first voltage step as the initial state occupancies for the next voltage step, etc. See Appendix for full description of the model used for the simulations shown in Figs. 10 and 11 (as well as for model parameters).

Solutions

All experiments were carried out using reduced Na solutions so as to maintain peak ionic current at less than ~1 mA/cm^2 under control conditions. The external perfusate typically contained (in mM): 75 Na, 13.5 Ca, 2.6 Mg, 135 TMA, 242.2 Cl, 2 Hepes; adjusted to pH 7.55. Adjustments of external sodium concentration were made by substitution of TMA for sodium ions. Internal perfusates usually contained (in mM): 0 Na, 0 K, 230 Cs, 60 F, 170 Glutamate, 1 Hepes; adjusted to pH 7.35. When recording gating currents without external TTX, internal Cs was substituted by TMA, following the method of Heggeness and Starkus (1986) who showed that gating current kinetics in crayfish axons are not affected by TMA at positive test potentials. Concentrations of Na, Cs, and TMA are listed in figure legends as external // internal (mM). All other components were constant in these solutions. Corrections were made for an electrode junction potential of 8–10 mV and electrode drift did not exceed 2–3 mV in these experiments.

RESULTS

Choice of initial conditions has been reported to affect both the magnitude and the apparent kinetics of gating currents (see Introduction). In this paper we attempt to clarify sodium channel gating mechanisms through selected changes in initial conditions. First, we examine effects on gating current kinetics of both (*a*) changes in holding potential and (*b*) prior inactivation by depolarizing prepulses. Our aim here was to provide, from crayfish axons, data comparable to the key findings which suggested gating current "fractionation" in squid axons (see Greeff et al., 1982; Bekkers et al., 1984; Keynes et al., 1990). Second, we examine additional experimental protocols designed to test the fractionation hypothesis. In both parts of this study we have included sodium current data obtained from the same experimental protocols, since additional information can be obtained from comparison of gating and ionic currents under identical conditions.

Effects of changes in holding potential

Changes in holding potential similarly affect both peak sodium current magnitude and gating charge (Q_t) in the absence of TTX (Heggeness and Starkus, 1986). The midpoint of the fully equilibrated gating charge distribution is at about −100 mV for crayfish axons in the presence of 200 nM TTX (Rayner and Starkus, 1989) but only −85 to −90 mV when gating currents are recorded without using TTX (see Heggeness and Starkus, 1986). However, the midpoint of the activation-related gating charge distribution obtained by integrating ON gating currents at different test potentials (the Q(V) curve), occurs at about −50 mV in these same axons (see Rayner and Starkus, 1989). These findings are consistent with a model developed by Bezanilla et al., (1982), in which the more negative midpoint of the fully equilibrated charge distribution (circa −85 mV) results from the progressive immobilization of the gating charges in their depolarization-favored position. Hence, the kinetics of IgON, reflecting the rate(s) at which gating charges leave their (nonimmobilizing) hyperpolarization-favored position, should be little affected by changes in holding potential (except for the small Cole-Moore delays seen by Taylor and Bezanilla, 1983). Bekkers et al. (1984) found no change in gating current kinetics for a shift in holding potential from −90 to −60 mV, which reduced by half the observed Q_t in their squid axons. Fig. 1 presents equivalent data for crayfish axons.

Fig. 1 *A* shows outward sodium currents recorded by stepping to a test potential of 20 mV from three different holding potentials. In comparison with the peak current recorded in the step from −120 mV (trace *a*), peak I_{Na} was reduced to ~50% at −85 mV holding potential (trace *b*) and to 25% at −77.5 mV (trace *c*). Holding potential was returned to −120 mV between traces *b* and *c* and following trace *c*, allowing control currents to be recorded (also at 20 mV test potential) to evaluate any rundown of I_{Na} occurring at the depolarized holding potentials. No such rundown was detected during these

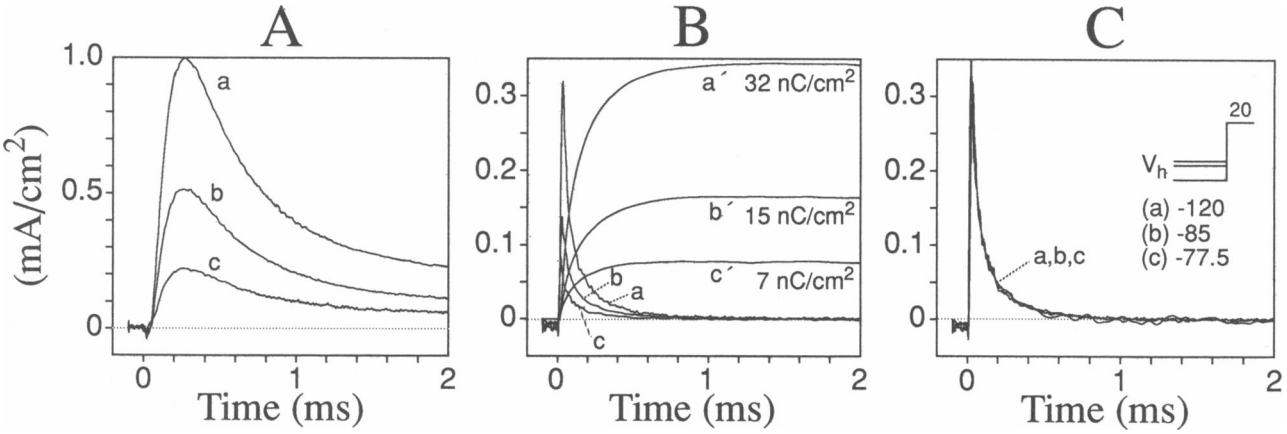

FIGURE 1 Changes in holding potential suppress both ionic current (*A*) and gating current (*B*) without affecting gating current kinetics (*C*). In each panel holding potentials were: trace *a*, −120 mV; trace *b*, −85 mV; trace *c*, −77.5 mV. All data from axon 900628. (*A*) Outward sodium currents recorded in 0 Na 200 TMA//25 Na 175 Cs. (*B*) Gating currents recorded in absence of TTX using 0 Na 200 TMA//0 Na 200 TMA. Traces *a'*, *b'*, and *c'* were obtained by integration of records *a*, *b*, and *c*, respectively. (*C*) Gating currents from *B* scaled to match control current magnitude at 100 μs after the start of the voltage step.

recordings. Cole-Moore-type shifts (cf. Hahin and Goldman, 1978; Taylor and Bezanilla, 1983) are not readily apparent in these records where half-activation times were 111 μs for trace *a*, 107 μs for trace *b* and 106 μs for trace *c*.

Fig. 1 *B* shows the equivalent gating currents (traces *a*, *b*, and *c*) and integration records (traces *a'*, *b'*, and *c'*) obtained from this same axon in the absence of TTX (following the method described by Heggeness and Starkus, 1986). In comparison with the total gating charge recorded in a step to 20 mV test potential from a holding potential of −120 mV (trace *a'*), Q_t was reduced to 47 and 22% at holding potentials of −85 and −77.5 mV (traces *b'* and *c'*), respectively. Both Q_t and peak I_{Na} appear similarly affected by changes in holding potential. The kinetics of these gating currents are compared in Fig. 1 *C*, where traces *b* and *c* have been scaled up to overlie trace *a* at 100 μs. All three gating currents overlie throughout their 2-ms duration; our results, thus, fully confirm the absence of effect of holding potential on gating current kinetics noted by Bekkers et al. (1984) and Heggeness and Starkus (1986).

The gating currents of crayfish axons were described as demonstrating three clear exponential components by Starkus et al. (1981). Similarly, recent studies of gating currents in squid giant axons have identified three major exponentials within the control Ig_t traces (Keynes et al., 1990). Exponential analysis (see Methods) of ten control gating currents recorded (at 20 mV) 3–5 min apart from the axon of Fig. 1, confirmed three statistically separable components with mean time constants (±SD) of 19 ± 6 μs, 89 ± 22 μs, and 310 ± 32 μs. However, our fitting routines were unable to resolve more than three statistically separable exponentials in these same traces. When these traces were analyzed as the sum of only two exponentials the quality of fit was substantially reduced and presence of an additional process was indicated by the waveform of the residuals (see Methods).

Effects of inactivating prepulses on IgON

Fig. 1 has demonstrated that gating currents can be markedly suppressed by depolarized holding potentials, without detectable changes in IgON kinetics. By contrast, the kinetics of IgON are altered (see Greeff et al., 1982) when equivalent suppressions of total charge movement are induced by inactivating prepulses. Fig. 2 *A* demonstrates this effect in crayfish axons. Holding potential was −120 mV and both prepulse and test pulse potentials were −20 mV. The interpulse interval was chosen as 0.3 ms (at −120 mV), for comparison with the standard 0.5-ms interval (at −80 mV) used by Greeff et al. (1982) and Keynes et al. (1990) in their prepulse protocols. Control gating currents (without prepulse) were inserted before (trace *a*, Q_t = 22.1 nC/cm²), during (not shown) and after the prepulse sequence (trace *f*, Q_t = 22.2 nC/cm²). Traces *b* through *e* show test pulse gating currents after prepulses of 0.5, 3, 20, and 30 ms duration, respectively. Gating charge integrated over a 3-ms period was reduced as prepulse duration increased (see Table 1). Thus, the apparent Q_n for 20- and 30-ms prepulses was about one-third of control Q_t in this axon, in good accord with observations of the "nonimmobilizable" fraction from other axons (see Introduction).

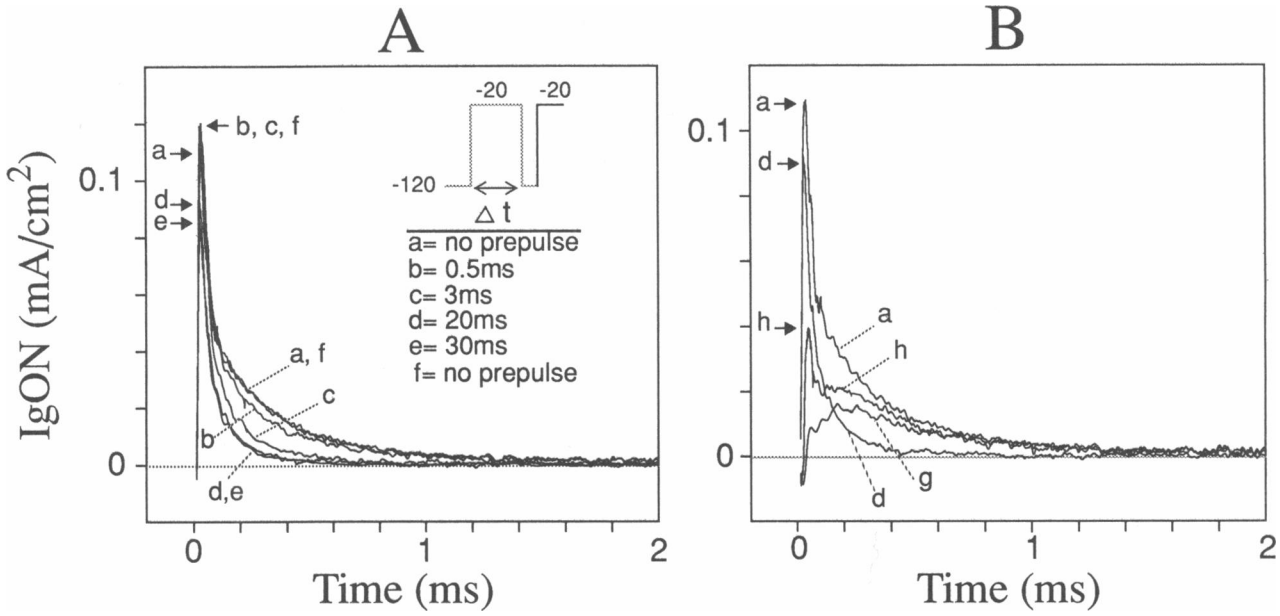

FIGURE 2 Inactivating prepulses suppress charge movement and alter IgON kinetics. Holding potential, −120 mV; both prepulse and test pulse to −20 mV. (Prepulse durations are shown in the pulse pattern insert.) Note: In all pulse inserts the full pulse pattern is diagrammed; the solid line indicates the voltage step for which records are shown. (*A*) Traces *a* and *f* are single pulse control gating currents recorded before and after, respectively, the series of double pulse records. Traces *b* through *e* were obtained at different prepulse durations (see inset). In each case the interpulse interval was 0.3 ms. Peak IgONs are indicated by horizontal arrows. (*B*) This panel repeats the control trace *a* and 30 ms prepulse trace *d* from *A*. The peaks of these record are identified to the left of the rising phase. We also show two "subtraction records" (see text). Trace *g* was obtained by subtracting trace *c*, after a 3-ms prepulse, from the control trace *a*; trace *h* was obtained by subtracting trace *d*, after a 20-ms prepulse, from trace *a*. Note the different rising phases of traces *g* and *h*.

The altered IgON kinetics after inactivating prepulses are made readily apparent by comparing the relative magnitudes of these gating currents at peak and at different times thereafter. Thus, at the time of peak IgON, trace *d* is 20% suppressed by comparison with the control (trace *a*). However, when these same traces are compared at 0.3 ms, trace *d* shows 80% suppression. Clearly, the slower components of the IgON are more readily suppressed by inactivating prepulses than the earlier and faster components.

TABLE 1 Effects of inactivating prepulses on Ig kinetics prepulse and test pulse to −20 mV; axon 870407

Conditions	Prepulse durations	Q_t*	τ_f	Q_f‡	τ_m	Q_m‡	τ_s	Q_s‡	*n*
Controls	*ms*	*nC/cm²*	*μs*	*nC/cm²*	*μs*	*nC/cm²*	*μs*	*nC/cm²*	
$\bar{x}$ ± SD		20	23.3 ± 1.9	1.4 ± 0.2	236 ± 23	10.1 ± 1.5	958 ± 404	7.2 ± 1.1	10
Short prepulse data									
	0.5	17.9	24.1	1.5	150	5.0	510	9.6	
	0.6	18.2	24.4	1.5	187	8.3	1020	6.9	
	0.8	16.4	26.5	1.8	177	7.0	685	6.0	
$\bar{x}$ ± SD		17.5 ± 1.0	25.0 ± 1.3	1.6 ± 0.2	171 ± 19	6.7 ± 1.6	739 ± 259	7.5 ± 1.9	3
Long prepulse data									
	10	9.0	31.7	1.7	142	4.7	1389	1.4	
	15	8.2	40.8	2.3	168	3.3	455	0.5	
	20	8.1	20.2	0.7	85	3.5	368	1.8	
	30	6.8	31.8	1.6	141	3.5	—	0.0	
	50	6.3	27.8	1.2	116	3.0	345	0.4	
$\bar{x}$ ± SD		7.7 ± 1.1	30.5 ± 7.5	1.5 ± 0.6	130 ± 31	3.6 ± 0.7	639 ± 502	0.8 ± 0.8	5

*From integration of Ig records. ‡From product of time constant and intercept (at 40 μm).

Exponential analysis of these gating currents again shows three well separated time constants (see Table 1). We compare mean data from ten control single pulse records with similar analyses of gating currents after "short" (0.5 to 1.0 ms) and "long" (10 to 50 ms) prepulses. Although progressive changes with increasing prepulse duration are detectable within both of these prepulse groups, we concentrated here on the general properties indicated by statistical comparisons between groups. First, the fast component appears to be insensitive to all prepulse durations shown here. Both charge movement (Q_f) and time constant (τ_f) are not significantly affected, despite the marked reduction in total charge movement (Q_t) occurring at longer prepulse durations. Similarly, there is no significant effect of prepulse duration on the slow component time constant (τ_s) although slow charge movement (Q_s) is reduced to only 10% of control at the longer prepulse durations. Both these results are consistent with expectations based on simple Markov models in which intercepts, but not time constants, can be expected to vary with changes in initial conditions. By contrast, the intermediate component shows highly significant changes ($P < 0.001$) in both charge movement (Q_m) and time constant (τ_m) between the control and long prepulse groups. This behavior is not compatible with any Markov model in which activation is represented as a simple sequence of three closed states and one open state (C-C-C-O) but is compatible with more complex models in which our "τ_m" might result from two (or more) closely spaced time constants which are differentially sensitive to prepulse inactivation. For example, if the slower of two hypothesized time constants were the more sensitive to prepulse inactivation, then the measured τ_m would appear faster after longer prepulse durations.

Comparison of control and long prepulse data in crayfish axons thus confirms the kinetic differences between Ig_t and Ig_n noted by Greeff et al. (1982) and Keynes (1983) in squid axons. However, such kinetic differences do not necessarily support the hypothesis that Ig_n is a separate entity generated in parallel with an immobilizable "Ig_i" component. The remainder of this paper examines that hypothesis from several different viewpoints.

First, we find that the subtraction method in crayfish axons does not yield such simple waveforms as were found in squid axons. Fig. 2 *B* compares the control gating current kinetics (trace *a*) from Fig. 2 *A* with traces obtained from two alternative subtraction procedures. Trace *h* in Fig. 2 *B* was obtained by subtracting the 20-ms prepulse record (trace *d*) from the control record (trace *a*). The slow rising phase seen in the subtraction records of Greeff et al. (1982) and Keynes et al. (1990) is not readily apparent in this trace. We find a fast initial peak at ~45 μs followed by an approximately biexponential relaxation containing two major components of 265 and 1163 μs. The sharp peak at 45 μs is not a chance result due to either noise or imperfect P/n subtractions. This peak, which is a constant feature in our subtraction records after long (>10 ms) inactivating prepulses, arises from the relative suppression of peak IgON which occurs at these prepulse durations. Peak IgON falls steadily for prepulse durations >3 ms, settling to an apparent asymptote of ~55 μA/cm² for prepulses between 500 ms and 2 s (not shown). Nevertheless, fast IgON disappears completely in test pulses initiated after 2 min at holding potentials more positive than −60 mV. Thus, the slow reduction in peak IgON described here appears related to the slow equilibration of the channel control mechanism seen by Rayner and Starkus (1989).

Noting that the initial sharp peak in trace *h* is caused by the relative suppression of peak IgON after a 20-ms inactivating prepulse, we have further explored this subtraction method using shorter prepulses where no significant reduction in peak IgON occurs. Trace *g* in Fig. 2 *B* was obtained by subtracting the 3-ms prepulse record (trace *c* of Fig. 2 *A*) from the trace *a* control record. A slow rising phase is now evident which peaks at ~170 μs, followed by a biexponential relaxation with time constants of 324 and 1449 μs. The two "difference currents" (traces *g* and *h*) thus show very similar relaxation kinetics. From the total of seven difference currents obtained for prepulse durations between 3 and 50 ms, we found time constants of 257 ± 60 μs and 857 ± 304 μs (mean ± SD). The slower of these time constants is not significantly different from the mean τ_s values in Table 1. Furthermore, Q_s was markedly reduced after long inactivating prepulses and should therefore be enhanced in the difference current. The faster rate (267 μs) is similar to the control τ_m (236 μs in Table 1) but is significantly slower ($P < 0.001$) than the τ_m of 130 μs remaining within the long prepulse Ig_n data.

We conclude that both Ig_t and Ig_n gating currents reflect the same eigenvalues, although with weighting factors (peak time intercepts) which vary with initial conditions. Thus, the intermediate relaxation time constant measured in our control gating currents, τ_m, apparently results from summation of two closely spaced exponential components: the slower of these (τ_{ms}) has a time constant of ~270 μs at −20 mV and is sensitive to prepulse inactivation (cf. the τ_{3b} of Keynes et al., 1990); the faster (τ_{mf}) has a time constant of ~130 μs at −20 mV and is relatively insensitive to prepulse inactivation. Nevertheless, within a general Markovian system, it remains possible that gating currents could result from: (*a*) movements of parallel, noninteractive, particles within a system such that movement of the immobilizable particle is delayed by some necessary prior reaction

(Keynes, 1986), (*b*) movements of parallel, noninteractive, particles where there is no such initial delay for the immobilizable particle or, (*c*) movements of particles which are so interactively coupled that given eigenvalues are not dominated by the kinetics of specific gating particles. A clear determination as to which of these alternatives provides the better explanation for our data could help to assess the important of allosteric or electrostatic coupling between the voltage sensors of the tetrameric sodium channel. At first sight, the complex waveform of trace *h* in Fig. 2 *B* would seem to argue against the possibility that this waveform accurately reflects the kinetics of the "immobilizable gating particle(s)." However, factors other than fast inactivation/immobilization might well affect the waveform of Ig_n, and hence contribute to the shape of the difference currents. The following sections therefore pursue a more complete understanding of the effects of prepulse inactivation protocols, so as to permit more definitive evaluation of the possible parallel origin of Ig_i.

1. *Is Ig_n generated by a separate subpopulation of noninactivating sodium channels?*

Fig. 3 shows outward sodium currents recorded from the same axon as the gating currents shown in Fig. 2 (immediately before addition of TTX). Traces *a* through *f* were obtained using the same pulse protocols as in Fig. 2. In Fig. 3 *A*, where the data traces are presented without TTX subtraction, it appears that sodium current is completely inactivated by prepulses longer than ~20 ms. However, in Fig. 3 *B*, subtraction of gating currents from these same traces reveals a clear rising phase in sodium current after both the 20 and 30 ms prepulses (traces *d* and *e*). Thus the "Ig_n" seen in traces *d* and *e* of Fig. 2 *A* was associated with detectable sodium channel gating, controlling this slowly inactivating component of TTX-sensitive sodium conductance.

Fig. 3 *B* (traces *d* and *e*) also demonstrates a continuing reduction in peak I_{Na} between 20 and 30 ms prepulse durations. By 20 to 30 ms after onset of a pulse to −20 mV, a squid axon would be considered to have settled to its "steady-state I_{Na}." As shown in Fig. 4, no comparable "steady-state" is identifiable in crayfish axons. Fig. 4 shows consecutive TTX-subtracted sodium currents recorded for three different durations (4, 80, and 400 ms in panels *A*, *B*, and *C*, respectively). Linear leak was removed by the capacity subtraction process and nonlinear leak was effectively removed by TTX subtraction; thus, no offset corrections have been applied to these records. Note the expanded vertical scales in 4 *B* and *C* required to show continuing decay of these outward currents. Further extension of the recording period to 2 s (not shown), clarifies that I_{Na} decays to less than 1 $\mu A/cm^2$ by 1.2 s. The two vertical arrows in Fig. 4 *B* indicate times comparable to the 20 and 30 ms prepulse durations used in Figs. 2 and 3, showing that I_{Na} is still inactivating at those prepulse durations. However, after a 20-ms prepulse, as much as 35% of Q_m remains nonimmobilized (see Table 1), although only 5% of peak

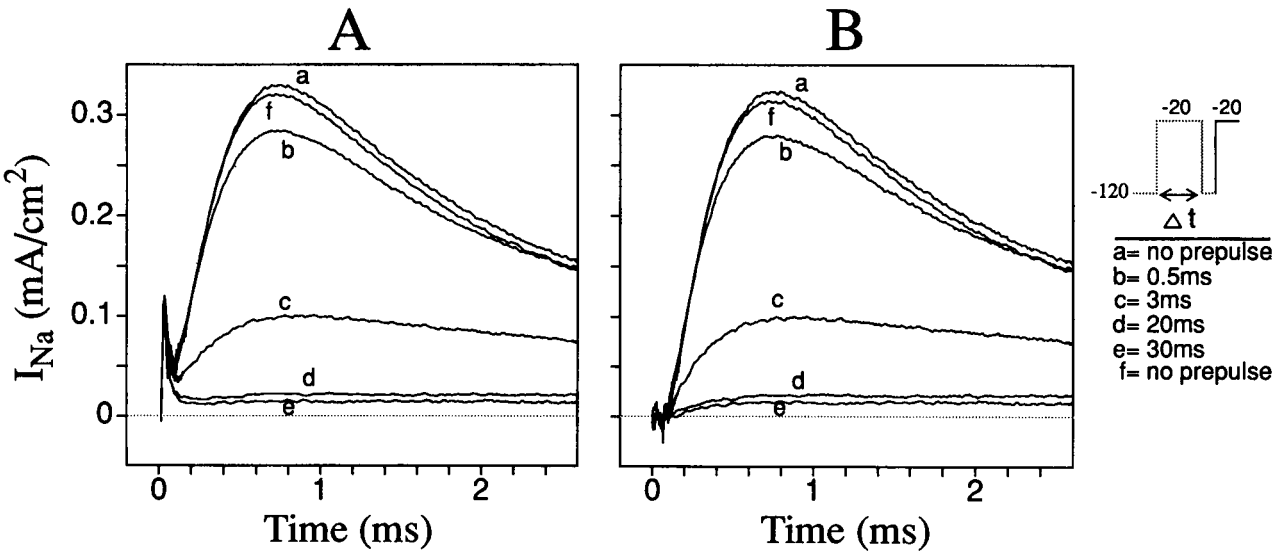

FIGURE 3 Inactivating prepulses also suppress peak I_{Na}. Prepulse parameters, test pulse and trace numbering are identical to Fig. 2 (see figure inset). (*A*) Outward sodium currents before gating current subtraction. Note no time-dependent outward sodium current is apparent in traces *d* and *e*. (*B*) Outward sodium currents after subtraction of gating current traces from this same axon shown in Fig. 2. Small outward currents are now apparent in traces *d* and *e* after prepulses of 20 and 30 ms, respectively. All data from axon 870407 in 0 Na 200 TMA//50 Na 150 TMA.

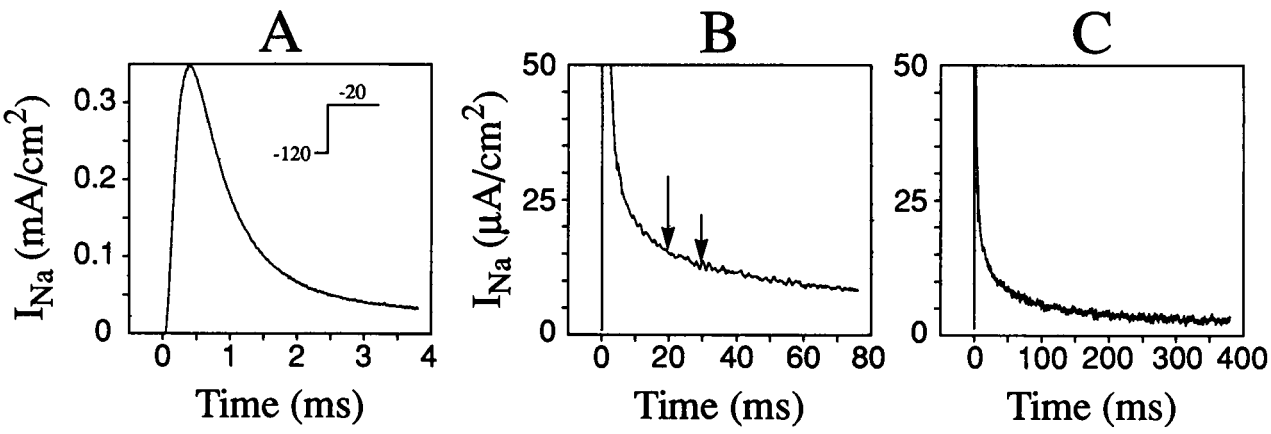

FIGURE 4 Sodium currents in crayfish axons show continuing slow decay without a recognizable plateau of "steady-state I_{Na}." TTX-subtracted outward sodium current from axon 86217 recorded in 0 Na 200 TMA//20 Na 180 Cs. All TTX-insensitive currents have been removed from these records by the TTX-subtraction procedure. (*A*) Data recorded at 1-μs sampling interval. (*B*) Data recorded at 20-μs sampling interval. Data scaled (note revised ordinate) to demonstrate continuing decay of sodium current. Vertical arrows indicate 20- and 30-ms points. (*C*) Data recorded at 100-μs sampling interval. Same ordinate scale as in *B*. Note continuing decay of outward sodium current to less than 5 μA/cm^2.

I_{Na} is noninactivated (compare traces *a* and *d* in Fig. 3 *B*). This inequality implies that "nonimmobilizable" gating charge cannot be merely the gating current from some separate population of noninactivating channels (unless these channels generate disproportionately large gating currents). It seems more reasonable to presume that less than 20% of Q_n arises from noninactivated channels. The remaining 80% of Q_n presumably represents a parallel, nonimmobilizable, component of gating charge generated within fast inactivated sodium channels.

2. *Do Cole-Moore-type shifts contribute to the kinetic changes induced by prepulse inactivation?*

Although large changes in sodium current magnitude are visible in Fig. 3 *B*, only minimal changes appear in the kinetics of I_{Na} activation (see below). These relatively constant I_{Na} kinetics should be contrasted with the marked changes on IgON kinetics seen in Fig. 2. Half-activation times for the control I_{Na} traces *a* and *f* in this figure were 286 and 282 μs. Traces *b* and *c* give 264 and 248 μs, respectively (currents were too small for accurate measurement of half-activation times in traces *d* and *e*). These small changes in half-activation times apparently reflect Cole-Moore-type lateral shifts in activation kinetics of, for example, ~34 μs in Fig. 3 *B*, trace *c*.

No such simple lateral shift is evident for the corresponding gating current records from this same axon (traces *a* and *c* in Fig. 2 *A*). Both gating currents have similar peaks that occur coincidently within the resolution of these experiments. However, when these traces are compared at a current magnitude of 60 μA/cm^2 (i.e., in the domain of the fast component of IgON) these two records can be made to overlap by a time shift of only 8 μs. When both gating currents further decrease with time, the lateral shift between these traces increases to 83 and 200 μs, where current magnitude is 30 or 15 μA/cm^2, respectively. As indicated by the complex "difference currents" shown in Fig. 2 *B* (traces *g* and *h*), the prepulse gating currents in Fig. 2 *A* cannot be aligned with control kinetics by a simple combination of scaling (to correct for charge immobilization, see Armstrong, and Bezanilla, 1974, 1977) and lateral shifting along the time axis (to correct for Cole-Moore-type time shifts in I_{Na} activation, see Taylor and Bezanilla, 1983). We conclude that Cole-Moore-type shifts are not the principal cause of the kinetic changes induced by protocols with equal test and prepulse voltages.

3. *Does slow inactivation contribute to the effects of inactivating prepulses?*

We have noted (see Fig. 4) that both fast and slow inactivation processes affect the time course of I_{Na} seen during long recording periods. It thus seems important to ask whether the fastest kinetics of slow inactivation can contribute to the effects of inactivating prepulses in the 20 to 30 ms range. Evidence that this is the case is provided by comparing the recovery rates of gating and ionic currents after 20-ms depolarizing prepulses (to −20 mV). Test pulse gating currents, also at −20 mV, are shown in Fig. 5 *A* for increasing interpulse intervals; outward sodium currents are shown in Fig. 5 *B*. Because individual peak gating currents are not readily resolvable in Fig. 5 *A*, the peak of trace *b* is marked by a horizontal arrow. Time to peak IgON was 20 μs for this trace, as compared with 32 ± 5 μs for a series of ten control traces. Note that the gating currents recover from the inactivation induced by the 20-ms depolarizing

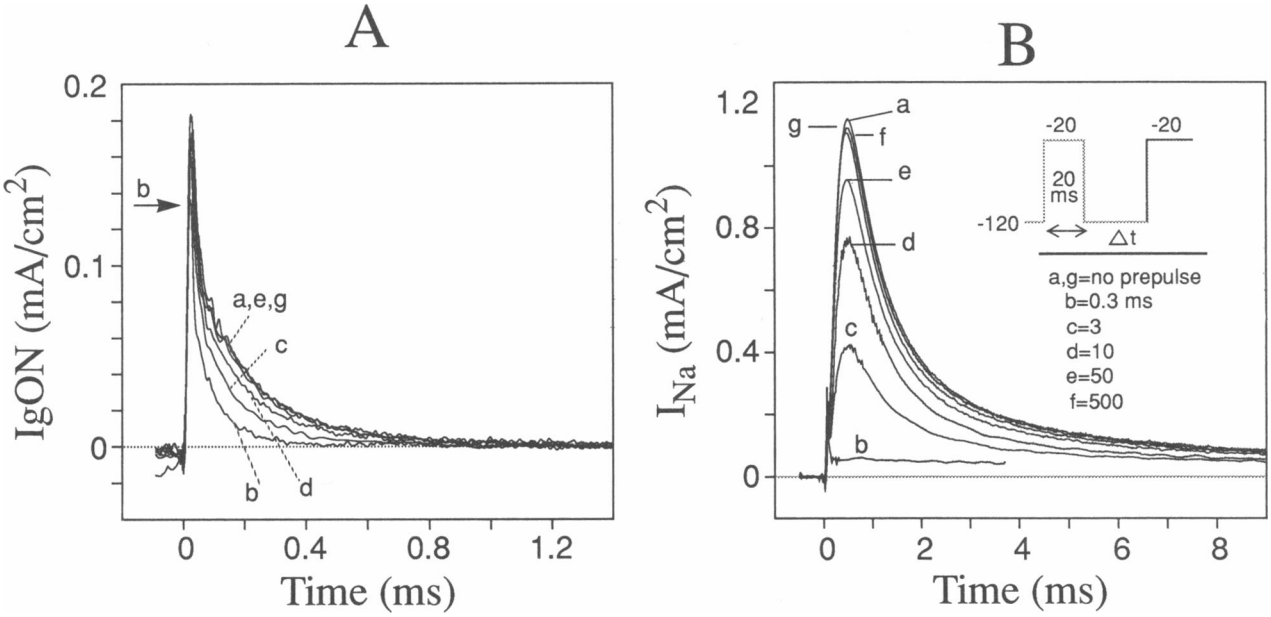

FIGURE 5 Effects of prepulse inactivation on gating current (*A*) and sodium curent (*B*) are progressively removed with increasing interpulse intervals at holding potential (−120 mV). Pulse parameters and trace numbering are the same in both panels (see inset). (*A*) Control gating currents (for single pulse from holding potential to test potential) are shown as trace *a*, before, and trace *g*, after, the sequence of double pulse records. Note records *a*, *g*, and *e* (after a 50-ms interval) overlie. Progressive recovery is evident in traces *b*, *c*, and *d* at 0.3, 3, and 10 ms, respectively. Note the reduced peak IgON, indicated for trace *b* by the horiziontal arrow to the left of the rising phase of IgON in this panel. Data from axon 870402 in 0 Na 200 nM TTX//0 Na 200 TMA. (*B*) Outward sodium currents are shown for the same interpulse intervals as in *A*. Note that recovery of peak sodium current was not complete in trace *e* after a 50-ms interpulse interval. However, essentially completely recovery is demonstrated in trace *f* after 500 ms at holding potential. Gating currents were not subtracted from these records. Data from axon 870409 in 0 Na 200 TMA//50 Na 150 TMA.

prepulse, regaining both control kinetics and control magnitude after ~50 ms at holding potential (see trace *e*). By contrast, the peak sodium current after this same 50-ms recovery interval (trace *e* of Fig. 5 *B*) reaches only 85% of control magnitude (trace *g*). Complete (>99%) recovery in Fig. 5 *B* required a 500-ms interpulse interval at −120 mV holding potential. A similar separation between recovery rates of gating and ionic currents has been noted both by Bezanilla et al. (1982) and Rayner and Starkus (1989) during recovery from depolarized holding potentials. We show here that this phenomenon can also be demonstrated after prepulses as short as 20 ms and conclude that significant (~15%) slow inactivation was induced at this prepulse duration.

We suggest that crayfish and squid axons may differ in that the fast components of slow inactivation (and slow immobilization) seem relatively faster in crayfish axons. Such a difference would expain the absence of a "steady-state I_{Na}" plateau in our records. Furthermore, effects of slow inactivation must sum with the effects of fast inactivation during long prepulses, possibly contributing additional components to "Ig_i" difference currents which might not be detectable in squid axons. Because a sharp peak appears in the difference current after a 20-ms prepulse (trace *h* of Fig. 2 *C*) but not after a 3-ms prepulse (trace *g*), we suspect that this difference current peak results from suppression of peak IgON by slow inactivation (compare peaks of traces *d* and *f*, identified by horizontal arrows in Fig. 2 *A*).

4. *Does interpulse interval affect the gating current kinetics seen in double pulse protocols?*

In view of the conclusion reached above, we may question whether clear separation can be achieved (in crayfish axons) between fast and slow inactivation by kinetic methods. In other words, if the fastest component of "slow inactivation" causes significant slow inactivation before "fast inactivation" can be considered complete, then these processes cannot be separated by appropriate choice of prepulse duration. However, they can be separated by pharmacological agents which remove fast inactivation without apparently altering slow inactivation rate. In the following section we address the effects of interpulse interval and prepulse duration after pretreatment with chloramine-T (Wang et al., 1985; Huang et al., 1987) for removal of fast inactivation.

More immediately germaine, however, is the critical question as to whether even activation and fast inactivation are truly separable by prepulse protocols. Introduced by Hodgkin and Huxley (1952*a*), the prepulse method involves a return to holding potential long enough to permit full recovery of the activation mechanism without significant change in the status of inactivation. But can activation and inactivation be reliably separated in this manner? Fig. 6 *A* suggests that they cannot. In this figure we compare the time course of a TTX-subtracted sodium tail current (trace *a*) with its equivalent IgOFF (trace *b*) after removal of fast inactivation with chloramine-T. For this return step to −120 mV (after a 1 ms step to 50 mV), both IgOFF and the sodium tail current reach a peak at the same time (26 μs) and show a fast relaxation which is completed in ~60 μs. However, both records also show a slower relaxation which continues in the original 4-ms data trace (not shown) for ~1 ms. If it takes as long as a millisecond for full return of Q_{OFF} even in the absence of charge immobilization, how could a full control Q_{ON} be expected after an interpulse interval of only 0.3 ms at −120 mV (as used here, see Fig. 2) or 0.5 ms at −80 mV (as used by Greeff et al., 1982; Bekkers et al., 1984 and Keynes et al., 1990)?

Fig. 6 *B* shows the effects of change in interpulse interval on IgON after removal of fast inactivation with chloramine-T. After a 2-ms prepulse to 0 mV, command potential was returned to holding potential for 0.05, 0.1, 0.4, and 1.0 ms in traces *a*, *b*, *c*, and *d*, respectively, before the final test pulse (also to 0 mV). Test pulse Q_{ON} was ~95% of control level after 1 ms at −120 mV. However, test pulse Q_{ON} was only 80% after 0.4 ms, 44% after 0.1 ms, and 27% after 0.05 ms. In the absence of fast inactivation, test pulse Q_{ON} is reduced by incomplete charge recovery during the brief returns to holding potential. This interpretation is readily visualized in Fig. 6 *B* where it is apparent that test pulse Q_{ON} is dependent on the amount of charge recovered during the preceding Q_{OFF}.

Fig. 6 *B* also demonstrates marked kinetic changes in test pulse IgON as a function of interpulse interval. These changes are similar to the kinetic changes occurring with increasing prepulse duration (see Fig. 2), except that here it is reduction in interpulse interval which apparently limits the slower components of IgON (rather than prepulse inactivation). When interpulse interval is as short as 0.05 ms (Fig. 6 *B*, trace *a*), only the fast component of IgOFF is completed in this very short return to holding potential. Note that the subsequent IgON is not a miniature version of the control IgON, as would be expected if all kinetic components of IgON

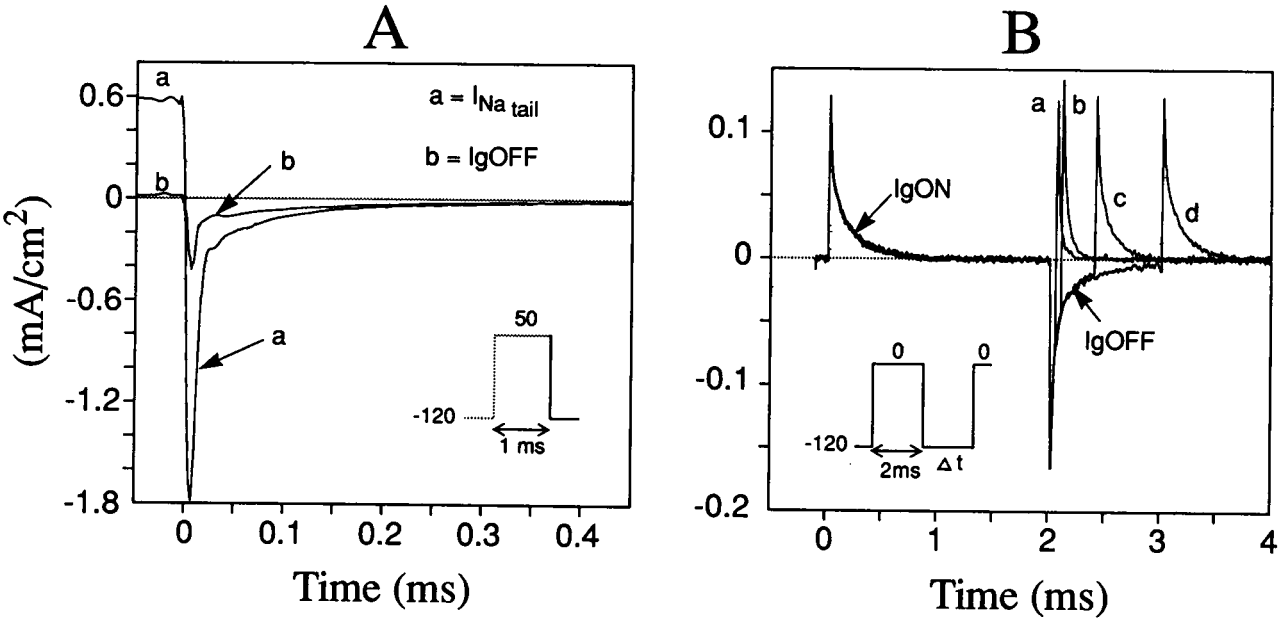

FIGURE 6 For short interpulse intervals, test pulse IgON is affected by the return rate of IgOFF, even at −120 mV and after removal of fast inactivation with chloramine-T. (*A*) Comparison of TTX-subtracted I_{Na} tail current (trace *a*) with IgOFF (trace *b*) recorded from the same axon under the same conditions. Note the similar kinetics of both records in the initial fast component as well as during the subsequent slow relaxation. Data from axon 890830 in 50 Na//25 Na 150 Cs after chloramine-T treatment. (*B*) Recovery of IgON kinetics with increasing interpulse interval after pretreatment with chloramine-T. Interpulse intervals were: trace *a*, 0.05 ms; trace *b*, 0.1 ms; trace *c*, 0.4 ms; and trace *d*, 1 ms. Data from axon 901128 in 0 Na 200 nM TTX//0 Na 200 Cs.

were equally represented within the fast IgOFF. By contrast, the subsequent IgON (in trace *a*) shows a predominant fast component with almost no detectable slower components. We therefore reach a most interesting conclusion, namely: the same "fast gating charges" generate both fast IgOFF and fast IgON. Similarly, the slower components of IgON only appear (see traces *c* and *d*) after increased interpulse intervals have allowed significant "slow charge" movement to become visible in the preceding IgOFF.

Fig. 7*A* shows similar gating current data from a different axon, again after pretreatment with chloramine-T. Here we have aligned the traces at the start of the test pulse to further expose the kinetic fractionation described above. At 0 mV test potential, single pulse control records indicated $\tau_f = 15.2 \pm 1.6$, $\tau_m = 174 \pm 7$, and $\tau_s = 832 \pm 348$ μs (mean ± SD, n = 4). The slow time constant was not detectable in the gating currents after 0.05- and 0.1-ms intervals at holding potential (traces *b* and *c*) but returned, showing ~50% of control slow charge, after the 0.4 ms interval ($\tau_s = 775$ μs in trace *d*). Furthermore, as we have previously noted for gating currents after prepulse inactivation (see Fig. 2), the intermediate charge movement after the shortest interpulse interval shows a significantly faster time constant than in the control traces. This faster time constant then recovers towards its control value with increasing interpulse interval. We found τ_m to be 79, 93, and 136 μs in traces *b*, *c*, and *d*, respectively. (Small differences in the fast components of these gating currents are not readily evaluated by exponential analysis.)

Comparison with our analysis of prepulse inactivation would suggest that the apparent change in time constant of the intermediate component might arise from relative suppression by short interpulse intervals of a slower intermediate subcomponent (τ_{ms}) which cannot be readily differentiated within our control gating currents. The difference current obtained by subtraction of the control and 0.05 ms records (see trace *c* of Fig. 10*B*) supports this interpretation. Analysis of this difference current indicates two major relaxations of 182 (τ_{ms}) and 417 μs (τ_s) which fully account for the later part of the control gating current. The faster intermediate time constant (τ_{mf}), measured in trace *b* as 79 μs, is not evident in the difference current and was apparently unaffected by the short interpulse interval. Thus the kinetic components which were more clearly suppressed by long inactivating prepulses (τ_s and τ_{ms}) are also, apparently, the components which are the most affected by short interpulse intervals.

Fig. 7*B* shows the sodium currents recorded from this same axon. After removal of fast inactivation with chloramine-T, only minor (~5%) rescaling was re-

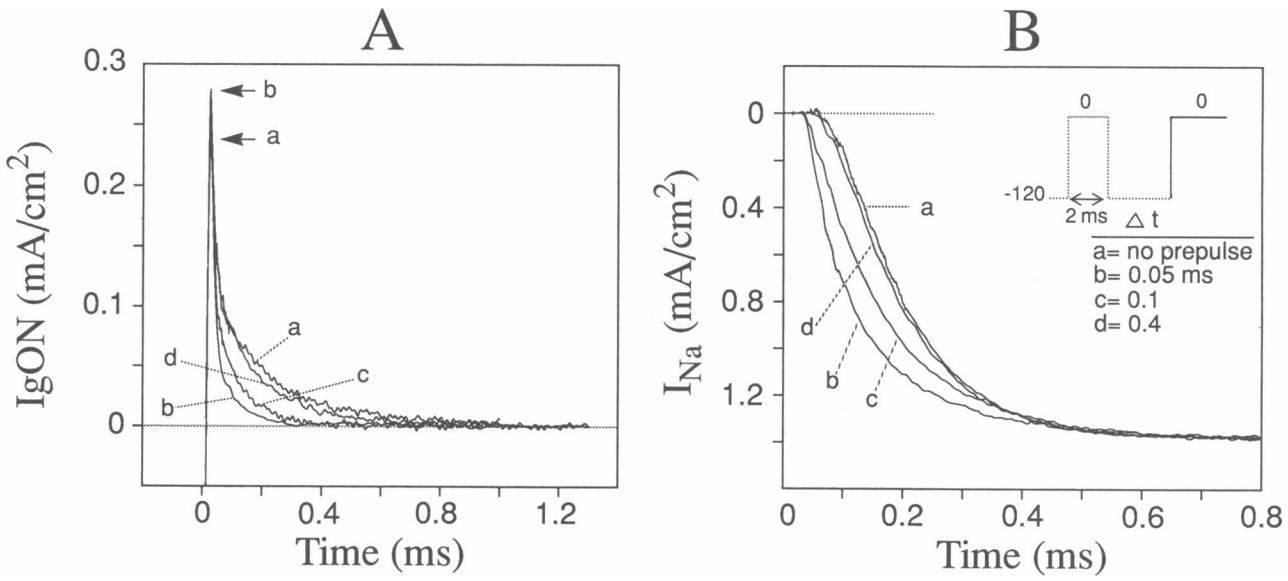

FIGURE 7 "Kinetic fractionation": the effects of short interpulse intervals on kinetics of IgON (*A*) and sodium current (*B*) in an axon pretreated with chloramine-T. (*A*) Comparison of control single pulse IgON, trace *a*, with IgON records after intervals of 0.05 ms, trace *b*; 0.1 ms, trace *c*; and 0.4 ms, trade *d*. Note that the peak of the 0.05-ms record is greater than the peak for the control single pulse record as indicated by the horizontal arrows. (*B*) Comparison of sodium current activation rate, see trace *a*, with sodium activation at different interpulse intervals (see inset). All data from axon 900816 in 75 Na 125 TMA//0 Na 200 Cs. Data for *B* was collected first, immediately before addition of 200 nM TTX to the external perfusate.

quired to correct for rundown in peak sodium current between traces *a*, *c*, and *d*. However, trace *b*, at the shortest interpulse interval (0.05 ms) required additional correction for the small fraction (~10%) of channels which had not closed during the brief preceding tail current (not shown). We note here that the first 50 μs of IgOFF closes some 90% of the sodium channels. Furthermore, when these same charges move as a greatly suppressed IgON (comprising no more than 25% of total gating charge), this IgON is sufficient to reopen all channels closed during the preceding IgOFF.

The kinetics of both IgON (Fig. 7 *A*) and sodium channel activation (Fig. 7 *B*) are affected by interpulse interval. For the longest interval shown here (0.4 ms, traces *d* in 7 *A* and 7 *B*) the change could be described as a simple lateral shift in both the IgON and I_{Na} records, comparable to the lateral shifts reported by Taylor and Bezanilla (1983). However, the data at shorter interpulse intervals cannot be so simply explained. For the gating currents of Fig. 7 *A*, comparing the 0.05-ms interpulse interval trace (*b*) with its control (trace *a*), the required time shifts would be 5 μs to align the currents at 0.15 mA/cm^2, and either 54 or 163 μs when gating current falls to 0.075 or 0.037 mA/cm^2, respectively. However, after the 0.4 ms interval, trace *d* appears identical to control between 0.15 and 0.075 mA/cm^2 and is significantly shifted only at 0.037 mA/cm^2 (where the shift is 36 μs from the control mean). Similarly, the sodium current rising phase was converted from the control sigmoid shape (trace *a*, Fig. 7 *B*) to an almost monoexponential rising phase in trace *b* at the shortest 0.05-ms interpulse interval (as noted by Oxford, 1982, who first studied this "secondary activation" process in squid axons). As the interval increases to 0.4 ms, sodium activation returns towards a Cole-Moore type parallel activation with a time shift of about 20 μs in this axon.

In conclusion, at short interpulse intervals return of gating charge after a depolarizing prepulse will be limited by the available time at holding potential. The slower kinetic components are selectively reduced in the test pulse IgON records of Figs. 6 *B* and 7 *A* at short (< ~1 ms) interpulse intervals. A similar effect must have occurred within the data of Figs. 2 *A* and 5 *A* where interpulse interval was only 0.3 ms. Thus the kinetic effects of inactivating prepulses seen in these figures must result from some combination of both "kinetic fractionation" and prepulse immobilization. For example, the suppression of Q_t seen at the short prepulse durations in Table 1 was only ~15%, although some 20% suppression of Q_t was noted for a 0.4-ms interpulse interval in Fig. 6 *B* (after removal of fast inactivation). Thus the effects of short (<1 ms) "inactivating" prepulses may be entirely accounted for by kinetic fractionation. By contrast, kinetic fractionation should have lesser effects on test pulse IgON at longer prepulse durations (>10 ms). Due to the faster OFF kinetics of nonimmobilizable "fast charge," the Ig_n estimated after a 20-ms prepulse should show little distortion from the short 0.3-ms interpulse interval.

Ig_i is not a separate parallel component of gating current

We have reported (see Alicata et al., 1989) that the peak of the fast component of control IgON occurs at ~30 μs in our axons, whereas integration of the capacity currents indicates that membrane potential settles within ~50 μs. These parameters retain similar values in the work reported here and, for example, peak IgON occurs at 36 μs in the control traces of Fig. 2. Clamp speed was monitored throughout these experiments by interspersed capacity current records (see Methods). Thus, the early sharp peak of the subtraction "Ig_i" trace noted at 49 μs in trace *h* of Fig. 2 *C* occurs as the clamp is finally settling, whereas the delayed rising phase suggested by the alternative subtraction record (trace *g* of Fig. 2 *C*) occurs long after membrane voltage has settled, at a time when the ionic current is already about half activated in these axons. Comparing the "Ig_i" traces *g* and *h* of Fig. 2 *C* with their comparable control gating currents shows that at the time of peak IgON in the controls, Ig_i is 0 in trace *g* and 30 μA/cm^2 in trace *h* (as compared with control peak IgON of 115 μA/cm^2). Thus, if the Ig_i difference currents accurately reflect the rise time of the immobilizable component of gating charge, then peak *Ig* should be essentially unaffected by changes in Ig_i magnitude induced by prepulse inactivation (for prepulse durations of 50 ms or less, where effects of slow inactivation are minimal).

We reasoned, however, that any possible coupling between fast inactivation and peak IgON would be exaggerated by very short interpulse intervals, where both "kinetic fractionation" and fast inactivation/immobilization would be affecting the gating currents. Of course, where the interpulse interval is far too short to permit full recovery of the activation mechanism, the effects of prepulse duration on peak IgON must be compared before and after pharmacological removal of fast inactivation. Fig. 8 presents the data obtained from the same axon before (Fig. 8 *A*) and immediately after (Fig. 8 *B*) removal of fast inactivation with chloramine-T. In Fig. 8 *A* (traces *b* and *c*) peak IgON falls rapidly concident with initial fast inactivation of I_{Na}, followed by a slower decline between 1 and 3 ms. In Fig. 8 *B*, after exposure to chloramine-T, the rapid early fall of peak IgON is not seen. However, these figures

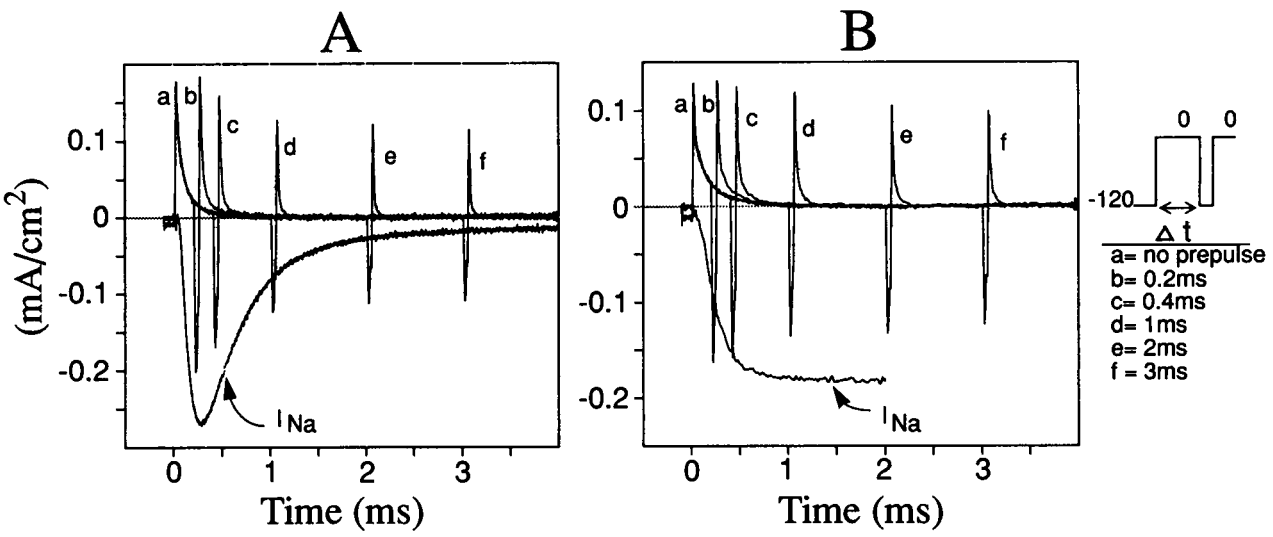

FIGURE 8 The effect of short prepulses on peak magnitude of IgOFF and IgON is altered by removal of fast inactivation with chloramine-T. *A* Shows gating currents and control sodium current with intact fast inactivation. *B* Shows gating currents and single pulse sodium current after chloramine-T treatment. See inset for prepulse durations. Interpulse interval was 0.05 ms throughout. I_{Na} records were obtained before addition of 200 nM TTX (*A*) and after TTX washout (*B*). Note equivalent changes in peak IgOFF and peak IgON in both panels. See text for further description of this figure. All data from axon 901204 exposed to 50 Na 150 TMA//0 Na 200 Cs.

serve to expose an additional problem which complicates direct visual analysis of our data. For prepulses shorter than ~1 ms, the prepulse terminates before ON charge movement is complete. Hence, the test pulse gating current will contain residual movements of "slow charge" (which did not yet leave its resting position during the brief prepulse). This residual "slow charge" sums with the fraction of nonimmobilized "fast charge" which forms the major contributor to test pulse peak IgON under these conditions.

Fig. 9 presents the data of Figs. 8, *A* and *B*, corrected for residual "slow charge" movement by subtracting off the value of the IgON at the end of the first pulse, (immediately before the return to holding potential). With fast inactivation intact (*filled symbols*), peak IgON falls rapidly during the first millisecond and continues to fall at a slower rate thereafter. With fast inactivation removed (*open symbols*), peak IgON increases until sodium current reaches its peak (at ~1 ms) and then falls slowly. This evidence rules against the hypothesized delayed rising phase of immobilizable Ig_i, by indicating a clear coupling between fast inactivation and peak IgON.

The important difference noted above between peak gating currents before and after removal of fast inactivation, should not overshadow the marked similarities between the results shown in Fig. 8, *A* and *B*. In both figures "kinetic fractionation", after a very short prepulse, markedly suppresses the slow component of IgON and both speeds and suppresses the intermediate component (apparently by selectively reducing the intercept of τ_{ms}).

DISCUSSION

The principal results of this study are:
(*a*) changes in holding potential equally affect all three

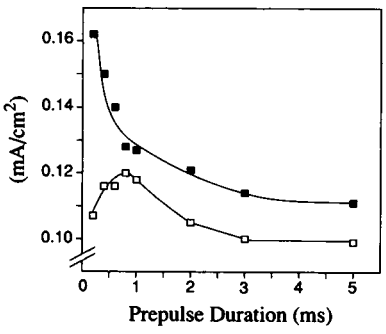

FIGURE 9 Effects of short prepulse durations on peak IgON before (*filled squares*) and after (*open squares*) removal of fast inactivation with chloramine-T. Data points were corrected for incomplete ON charge movements during the brief prepulses used here (see text). All data from axon 901204 as shown in Fig. 8.

major kinetic components of gating current (see Fig. 1 *B* and *C*, also Bekkers et al., 1984);
(*b*) prepulse inactivation of IgON reduces charge moving in the intermediate and slow components by about two-thirds. Furthermore, the intermediate relaxation rate, measured after ~30 ms depolarizing prepulses, appears significantly faster than in single pulse control gating currents. Fast gating charge is not reduced by prepulse inactivation (see Table 1);
(*c*) the "nonimmobilizable" component of gating current occurs together with gating of a small slowly-inactivating component of sodium current (see Figs. 3 *B* and 4);
(*d*) change of interpulse interval affects the IgON kinetics obtained using the prepulse protocol. After removal of fast inactivation with chloramine-T, we find that interpulse intervals > 1 ms are required for full recovery of control IgON (see Fig. 6 *B*). Intervals shorter than ~1 ms prevent the return of slower moving gating charges within IgOFF (see Figs. 6 *B*, 8 *A*, and *B*), causing suppression of the slower kinetic components of subsequent test pulse IgON (see Fig. 7 *A*);
(*e*) using very short interpulse intervals (0.05 ms), we demonstrate that peak IgON is reduced by fast inactivation (see Figs. 8 *A* and 9).

Effects of initial conditions on gating current kinetics

We have confirmed here that effects of initial conditions on gating current kinetics extend beyond partial immobilization of gating charge (Armstrong and Bezanilla, 1974, 1977) and lateral "Cole-Moore type" shifts in IgON kinetics (Taylor and Bezanilla, 1983), to include marked changes in the apparent IgON relaxation rates, as reported by Keynes et al. (1990). The possible significance of these findings is discussed below.

Parallel and sequential processes in channel gating. When attempting to assess the contribution of parallel mechanisms to the gating currents, it is important to distinguish clearly between structural and kinetic concepts of "parallel" action. The structural parallelism inherent in a pseudosymmetrical tetrameric channel need not necessarily lead to parallel kinetic behavior. For example, a "tetrameric" gasoline engine contains four parallel cylinders, yet these cylinders are constrained to follow strictly sequential kinetics through the allosteric coupling provided by the crankshaft and its associated timing mechanisms. In such a system, reaction order is mechanically determined and invariable. By contrast, in a kinetically parallel system no coupling exists and reaction order is only statistically determinable. Between these simple extremes, a realm of possibilities can be predicted in which partial kinetic coupling between structurally-parallel voltage sensors may generate more complex kinetic behavior.

Recent work further suggests that the final step in channel opening may be voltage insensitive. Evidence favoring this possibility has been presented by Zagotta and Aldrich (1990) for potassium A-channels and by Alicata et al. (1990) for sodium channels in crayfish axons. Additionally, Zimmerberg et al. (1990) have shown that osmotic stress affects the open probability for delayed rectifier channels in squid axons. Their results suggest that potassium channels must be hydrated in order to conduct permeant ions, becoming nonconducting if they lose their waters of hydration. These authors suggested alternative parallel and sequential models for the relationship between the voltage-sensitive and solvent-sensitive (but voltage-insensitive) gating processes.

We note the very substantial structural evidence suggesting four primary voltage sensors, one within each domain of the tetrameric channel molecule (see, for example, Montal's 1990 review). Furthermore, Stuhmer et al. (1989) have shown that mutation within sodium channel S4 segments can affect the voltage-sensitivity of sodium channel activation. Accepting that the sodium channel probably contains four structurally parallel voltage sensors, the major issues must be: (*a*) how many of these sensors are involved in channel activation (as opposed to fast and/or slow inactivation), (*b*) to what extent are these voltage sensors cross coupled (by allosteric or coulombic interactions), and (*c*) to what extent are voltage sensor kinetics affected by coupling to other voltage-insensitive gating processes (such as channel hydration and/or fast inactivation)? The data presented here permits some progress towards answering these questions.

Fast IgON reflects a parallel component related to sodium channel gating. Bekkers et al. (1989) suggested that the small fast component of IgON (~1 nC/cm^2 in their data, see also Keynes et al., 1990) might be a separate entity with no necessary relationship to sodium channel gating. However, if that were the case, why should this component remain in constant proportion to the slower gating components after changes in holding potential (see Fig. 1)? In the following paragraphs we develop an additional argument to suggest that the fast component of IgON reflects a parallel sodium channel gating mechanism.

The fast component of IgOFF relaxes at a rate essentially identical to the prominent fast relaxation in sodium tail currents from both *Myxicola* (see Goldman, 1991) and crayfish axons (see Fig. 6 *A*). Fig. 6 *A* shows ~85% of channels closing coincident with a fast IgOFF of 1.1 nC/cm^2, where the fraction of closing channels

(F_c) is calculated as:

$$F_c = (\text{peak tail current} - \text{slow intercept})/\text{peak tail current}.$$

Although it may seem surprising that so large a fraction of channels could be closed by so small a charge movement (total Q_{OFF} was 24.4 nC/cm^2 in that axon), the similarity of the fast IgOFF and fast tail current rates (both time constants are ~5 μs in Fig. 6*A*) after removal of fast inactivation with chloramine-T makes it difficult to reach any other conclusion. Thus fast IgOFF appears coincident with a readily demonstrable channel gating process, which Goldman (1991) has elegantly argued must reflect the first deactivation reaction in any linear scheme.

We have seen (see Figs. 6*B* and 8, *A* and *B*) that when interpulse interval is very short (~50 μs), comparable to the duration of the fast IgOFF at −120 mV, then both OFF and ON gating currents must result from movement of the same "fast changes." Moreover, our data shows no sign of discontinuities in fast IgON as interpulse interval is extended from 0.05 ms to 1 ms and we see no reason to doubt that the same "fast charges" are moving in all the ON gating currents in these figures, regardless of the preceding interpulse interval. In addition, fast IgOFF is quantitatively similar to fast IgON in our data (both range between 1 and 2 nC/cm^2 at the test potentials used here). As Bekkers et al. (1984) have pointed out, it is incompatible with sequential kinetic models that the same charges should be the first to move in both ON and OFF voltage steps. We conclude, therefore, that the fast components of both IgON and IgOFF reflect a parallel "fast gate" which is not immobilizable by fast inactivation.

Although fast inactivation reduces peak IgON as seen in Figs. 2*A*, 5*A*, 8*A*, and 9, our analyses indicate that the amount of charge moving in the fast component of IgON was not significantly affected (Table 1). The peak magnitude of IgON falls primarily by reduction of the peak-time intercepts for the slower charge components (τ_{ms} and τ_s), which form a variable "pedestal" beneath the fast kinetic component (see Figs. 8*A* and 9). The "fast component" described here (from exponential analysis) thus differs from the experimentally-determined parallel Ig_n noted by Greeff et al. (1982) and Keynes (1983), because their Ig_n includes the substantial additional charge moving in the faster intermediate subcomponent (τ_{mf}) after long inactivating prepulses (see Table 1). It is not clear from our analysis whether τ_{mf} should be regarded as a separate kinetic of "fast charge" movement or as indicative of an additional parallel process which is also resistant to immobilization by fast inactivation.

The origin of the changes in the intermediate IgON relaxation rate. We have demonstrated statistically significant changes in the intermediate gating current relaxation rate, after both inactivating prepulses (see Table 1 and Figs. 2*A*, 5*A*) and changes in interpulse interval (see Fig. 7*A*). We suggest that these apparently changing time constants result from selective changes in the weighting factors of different eigenvalues, within a more complex kinetic system than is demonstrable with available analytical methods.

We have explored this possibility (see Results) through careful analysis of data from the experiment illustrated in Fig. 2. At −20 mV test potential it appears that the 240-μs intermediate time constant (τ_m), found in our three component analyses of control IgON, primarily reflects the larger charge movement associated with the 270-μs immobilizable component (seen in analyses of difference currents) rather than reflecting the approximately twofold smaller 130-μs nonimmobilization component (seen in long prepulse data). When the original control record is reconstituted by addition of the difference current and the long prepulse record (e.g., by addition of traces *c* and *g* to obtain trace *a* in Fig. 2*B*) then only the single 240-μs time constant is recognized by our analysis programs. Four component analysis was unable to resolve this small (twofold) difference in time constants in the control records, particulary in view of the disparity in weighting between these two closely spaced time constants. Analysis of difference currents thus facilitates detection of closely spaced time constants, provided that experimental situations are used which differentially affect their weighting factors.

The relationship between IgON and I_{Na} activation. Our data, after removal of fast inactivation (see Figs. 7, *A* and *B*, and 8*B*), offer opportunities for comparisons between gating and ionic current kinetics which have not been explored here. Additionally, the comparative kinetics before and after removal of fast inactivation (see Fig. 8*A* and *B*) should provide additional information as to the coupling between activation and fast inactivation/immobilization. However, such detailed comparisons of IgON and I_{Na} kinetics may become more productive after our presentation of an approach which permits improved kinetic resolution in the analysis of IgON. For example, as seen in Fig. 7*B*, the rate of rise of I_{Na} increases during secondary activation (trace *b*) as compared with primary activation (trace *a*), Similarly, the gating currents (Fig. 7*A*) show an equivalent shift towards τ_{mf} during secondary activation (trace *a*) as compared with primary activation (trace *b*) where the intermediate time constant is dominated by τ_{ms}. If τ_{mf} and τ_{ms} are later found to have different voltage sensitivities, such distinctions could help to resolve the apparent

discrepancy noted by Goldman (1991) between the voltage sensitivities of his two resolved IgON time constants and his "τ_m" derived from the rising phase of I_{Na}.

Computer simulations of kinetic fractionation

The analysis undertaken here provides evidence for at least four kinetic components within the gating currents: the fast (τ_f) and slow (τ_s) components of IgON, and the two time constants (τ_{mf} and τ_{ms}) which contribute to the intermediate component in control gating currents. Although all four components appear equally affected by slow immobilization (see Fig. 1), only the two slower components (τ_{ms} and τ_s) are suppressed by both prepulse inactivation (Fig. 2) and short interpulse intervals (Figs. 6 *B* and 7 *A*). It would be tempting to assume that these four analytical components reflect the four independent voltage sensors implicit in the tetrameric structure of the sodium channel (cf. Catterall, 1986; Keynes, 1990).

By contrast, we explore here a more parsimonious model which provides reasonable simulations of our kinetic fractionation data although presuming that only two voltage sensors are required to control activation/deactivation in sodium channels. We first assume that the solvent-sensitive, voltage-insensitive process which Alicata et al. (1990) found to be rate limiting during primary activation reflects a "slow" channel hydration step equivalent to that noted by Zimmerberg et al. (1990) in delayed rectifier channels. Given the osmotic work to be overcome during channel opening, we have made explicit the coupling between voltage-sensitive and solvent-sensitive processes inherent in the sequential model presented by Zimmerberg et al., by assuming that a higher valence "intermediate gate" drives the solvent-sensitive channel hydration step via electrostatic coupling. Finally, our data has suggested the presence of a parallel, lower valence, "fast gate." This particle would be important in closing channels during fast deactivation but would fail to open channels during normal activation, when the additional parallel gating mechanisms described above should be rate limiting. Our model thus explores the behavior of two parallel but nonidentical voltage sensors (see Ruben et al., 1990) as well as the effects of coupling between voltage-sensitive and voltage-insensitive gating processes. However, we have not yet included the additional coupling to fast inactivation which should permit simulation of our prepulse inactivation data. (See Appendix for a complete description of the eight-state model which results from this formulation.)

Fig. 10 *A* shows a simulation obtained using this model for comparison with the replotted experimental data from Fig. 7 *A* (see Fig. 10 *B*). Both panels show control IgON (traces *a*), IgON after a 0.05-ms interpulse interval (traces *b*), and the difference currents (traces *c*) obtained by the subtraction method. Both difference currents show a delayed rising phase. Furthermore, in the model just as in the experimental data, the slower components of IgON appear selectively suppressed at short interpulse intervals. However, for the simulated data, the mechanism of this suppression can be further examined as described below. Using the Matlab programs to evaluate the matrix of rate constants for this model, we obtained seven nonzero reciprocal eigenvalues: 4.6, 8, 39, 43, 76, 119, and 441 μs at 0 mV test potential. Nevertheless, our analytical programs, detected only three time constants in the simulated control IgON:15, 79, and 473 μs. By comparison, exponential analysis of the simulated IgON after a 0.05-ms interpulse interval showed a slow tau of 322 μs (with a markedly reduced intercept) and a fast tau of ~9 μs. Interestingly, the intermediate tau was speeded to 49 μs (from 79 μs in the control simulation), comparable to the apparent speeding of τ_m in the equivalent experimental data (Figs. 7 *A* and 10 *B*). It seemed likely that this apparent change in rate resulted from selective suppression of the slower 119 and 441 μs time constants (relative to the 39 and 43 μs time constants). We examined that interpretation by analyzing the "difference record," trace *c* in Fig. 10 *A*. The slow tau (here 493 μs) is readily apparent, while the intermediate tau was 87 μs, consistent with our suggestion that the slower 119 and 441 μs components were selectively suppressed after interpulse intervals too short to permit significant return to the closed (dehydrated) state of the solvent-sensitive gating mechanism.

In this model, the rising phase of the difference current does not reflect a delayed rising phase for that component of total gating current which is generated by the intermediate (immobilizable) particle. The slower rise time of the simulated difference current results merely from increased intercepts of the faster time constants, after short interpulse intervals.

CONCLUSIONS

Our work demonstrates a detailed correspondence between squid and crayfish gating currents. The immobilizable components in our crayfish gating currents, τ_{ms} and τ_s, appear equivalent to the τ_{3b} and τ_4 noted by Keynes et al. (1990). Similarly, the components which are least affected by 20-ms prepulses in crayfish axons, τ_f and τ_{mf}, seem comparable to their nonimmobilizable τ_1, τ_2, and τ_{3a}.

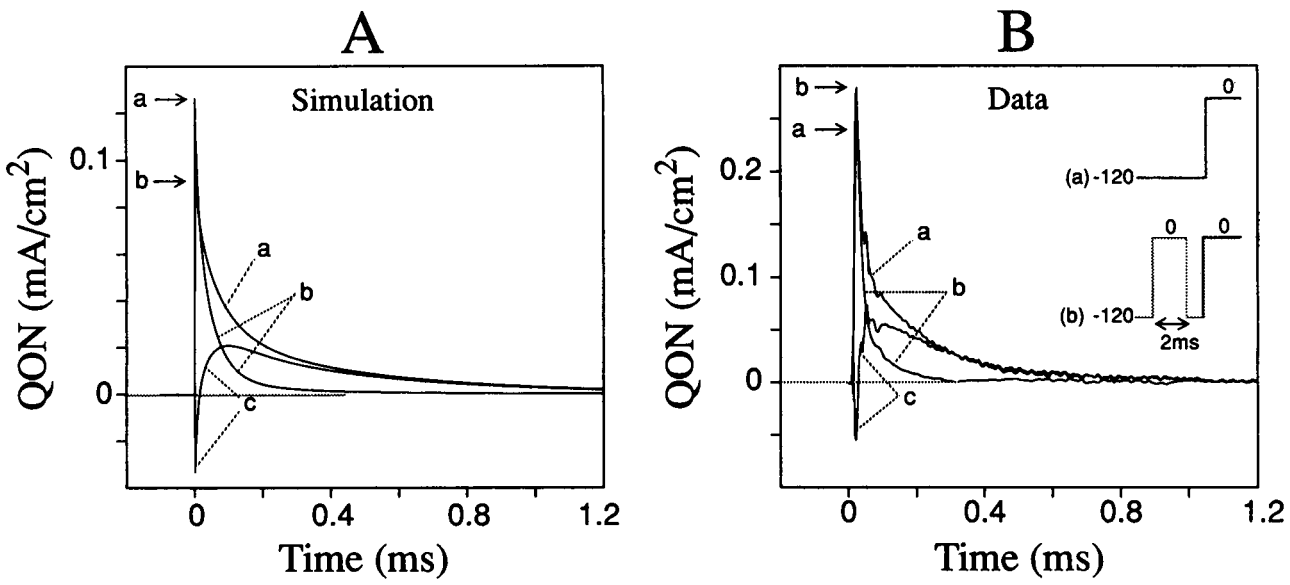

FIGURE 10 "Kinetic fractionation": difference currents obtained by the subtraction method for simulated data (*A*) and comparable experimental records from Fig. 7 *A* (*B*). (*A*) Subtraction of the 0.05-ms interval simulation (trace *b*) from the single pulse control simulation (trace *a*) gives the "difference current" (trace *c*). (*B*) Subtraction of the experimental 0.05-ms interval record (trace *b*) from the single pulse control record (trace *a*) gives an equivalent "difference current" for the experimental data. Note the initial peak is a downward deflection in trace *c*, identified by the labeled horizontal line, which is followed by a slower two-component relaxation. For these experimental records, the difference current (trace *c*) exactly matches the control record (trace *a*) at all times longer than ~250 ms.

By contrast, our careful study of the effects of prepulse inactivation does not confirm that the apparent slow rising phase of Ig_i-type difference currents results from a delay in the rise of the immobilizable component of IgON. Prepulse inactivation can reduce peak IgON, indicating a substantial contribution to peak IgON from immobilizable components of charge movement. Nevertheless, we find that in both the simulated and experimental data, difference currents obtained by the subtraction method permit assessment of the selective effects of initial conditions on different analytical components within kinetically complex gating mechanisms. Difference currents can thus provide potentially useful "fractionation" of the gating currents, although in a somewhat different sense than Greeff et al. (1982) first claimed. It thus seems time to reject an opinion we have previously held: that "Ig_i-type" difference currents are of interest only if they can be proven to reflect behavior of a separate, noninteracting, parallel gating charge. Just as the TTX-subtraction method clarifies the kinetics of I_{Na} onset, so difference gating currents may help to clarify the kinetic effects of changes in initial conditions.

Finally, although our data cannot yet distinguish amongst the range of interactions possible between structurally-parallel voltage sensors, at least two parallel, noninteracting, components of charge movement have been identified here. Furthermore, a model which includes explicit electrostatic coupling (of only about one-tenth kT) between one of these components and a voltage-insensitive slow gating mechanism (equivalent to the solvent-sensitive process proposed by Zimmerberg et al., 1990), generates IgON kinetics very similar to those seen in experimental data from both squid and crayfish sodium channels.

APPENDIX

The model used here in simulations of gating current kinetics (see Fig. 10 *A*) is a modified version of the eight-state model originally developed by Bezanilla et al. (1982) to describe electrostatic coupling between a single voltage sensor and two voltage-insensitive immobilizing processes. Here, we adapt that model to describe three parallel gating mechanisms: two independent voltage-sensitive gates, one of which is electrostatically coupled to a voltage-insensitive process by which channels enter into their hydrated, potentially conducting, conformation. Thus, an open channel will close when it loses its waters of hydration or when any either voltage sensor moves into its "closed" position. By contrast, a channel only opens when both voltage-sensitive gates are in their "open" configuration and the channel has been hydrated. However, because our formulation closely follows the approach used by Bezanilla et al. (1982) and Rayner and Starkus (1989), we repeat here only the minimum information required to fully specify the present model.

Presuming each of the three gating processes to be a first-order reaction yields an eight-state kinetic model in which electrostatic coupling is represented as a change in well-to-barrier height. Thus, all reactions leading out of the *i*th state will be affected by the appropriate

coupling term (W_i), following the convention that attraction between particles is represented by negative coupling which increases well-to-barrier height. The "uncoupled" nature of the parallel fast particle is represented in this scheme by ensuring symmetrical coupling energies for the forward and backward rates of this particle. Rate equations and parameters for each reaction are provided below. Our numbering convention assumes state 1 to be the major resting state whereas state 8 is the only open state. All voltage steps were presumed instantaneous.

The voltage-sensitive transitions

Voltage-sensitive reaction rates are calculated using the modified rate equations introduced by Bezanilla et al. (1982). Thus, K_α and K_β are:

$$K_\alpha = (kT/h) \cdot \exp(-w_a - ezxV/kT) \cdot \exp W_a$$
$$K_\beta = (kT/h) \cdot \exp(-w_b + ez(1-x)V/kT) \cdot \exp W_b,$$

where w is the height of the energy barrier (in kT units) as seen from well a or b, respectively, e is the electronic charge, z is the effective valence of the transition, V is the applied membrane potential, x is the fraction of the reaction coordinate at which the peak of the energy barrier occurs and all other symbols are as previously defined or have their conventional significance.

(*a*) *The fast particle.* We assume that this reaction involves the following state transitions: 1,5; 2,6; 3,7; and 4,8. Parameters used were w_a, 19; w_b, 20; z, 0.5; x, 0.5.

(*b*) *The intermediate particle.* For the same voltage dependent rate equations as defined above, parameters were: w_a, 20.2; w_b, 23.8; z, 1.5; x, 0.5. We assume this reaction involves transitions: 1,2; 3,4; 5,6; 7,8.

The solvent-sensitive transition

Where there is no necessity to evaluate effects of changing osmotic stress on the behavior of the system, the voltage-insensitive rates of the solvent-sensitive reaction can be expressed by the rate constants γ and δ such that:

$$K_{a,b} = \gamma \cdot \exp W_a$$
$$K_{b,a} = \delta \cdot \exp W_b,$$

where W_a and W_b are the coupling energies for the dehydrated (1, 2, 5, and 6) and hydrated channel states, respectively.

The transitions identified with the solvent-sensitive hydration process were: 1,3; 2,4; 5,7; and 6,8. The rates used (in reciprocal μs) were $\gamma = 0.00134$ and $\delta = 0.00174$.

Coupling energies

The coupling energies (in kT units) used for these simulations were: W_1 and W_5, -1.5; W_2 and W_6, 1.5; W_3 and W_7, 0.75; W_4 and W_8, -0.75.

We thank Dr. P. C. Ruben and Dr. D. A. Alicata for their assistance and encouragement throughout this project. We are particularly grateful for the constructive comments offered by Professor R. D. Keynes after reading a draft version of this manuscript.

Our work was supported in part by National Institutes of Health grant NS-21151, by award G12RR-03061 to the University of Hawaii under the Research Centers in Minority Institutions program of NIH, and BRSG 2S07 RR-07026 awarded by the Biomedical Research Support Grant Program, Division of Research Resources. Additional support was received from the University of Hawaii Research Council and the American Heart Association (Hawaii Affiliate).

Received for publication 9 January 1991 and in final form 15 July 1991.

REFERENCES

Alicata, D. A., M. D. Rayner, and J. G. Starkus. 1990. Sodium channel activation mechanisms: insights from deuterium oxide substitution *Biophys. J.* 57:745–758.

Alicata, D. A., M. D. Rayner, and J. G. Starkus. 1989. Osmotic and pharmacological effects of formamide on capacity current, gating current, and sodium current in crayfish giant axons. *Biophys. J.* 55:347–353.

Armstrong, C. M., and F. Bezanilla. 1974. Charge movement associated with the opening and closing of the activation gates of the Na channels. *J. Gen. Physiol.* 63:533–552.

Armstrong, C. M., and F. Bezanilla. 1977. Inactivation of the sodium channel. II. Gating current experiments. *J. Gen. Physiol.* 70:567–590.

Armstrong, C. M., anD D. R. Matteson. 1984. Sequential models of sodium channel gating. *Curr. Top. Membr. Trans.* 22:331–352.

Bekkers, J. M., N. G. Greeff, R. D. Keynes, and B. Neumcke. 1984. The effect of local anesthetics on the components of the asymmetry current in the squid giant axon. *J. Physiol (Lond.).* 352:653–668.

Bekkers, J. M., I. C. Forster, and N. G. Greeff. 1989. High resolution recording to Na gating currents from squid reveal a fast initial component. *Biophys. J.* 55:316a.

Bezanilla, F., R. E. Taylor, and J. M. Fernandez. 1982. Distribution and kinetics of membrane dielectric polarization. I. Long-term inactivation of gating currents. *J. Gen. Physiol.* 79:21–40.

Bullock, J. O., and C. L. Schauf. 1978. Combined voltage-clamp and dialysis of *Myxicola* axons: behavior of membrane asymmetry currents. *J. Physiol. (Lond.).* 278:309–324.

Catterall, W. A. 1986. Voltage-dependent gating of sodium channels: correlating structure and function. *TINS.* 9:7–10.

French, R. J., and R. Horn. 1983. Sodium channel gating: models, mimics, and modifiers. *Annu. Rev. Biophys. Bioeng.* 12:319–356.

Goldman, L. 1991. Gating current kinetics in *Myxicola* giant axons. *Biophys. J.* 59:574–589.

Greeff, N. G., R. D. Keynes, and D. F. van Helden. 1982. Fractionation of the asymmetry current in the squid giant axon into inactivating and non-inactivating components. *Proc. R. Soc. Lond. B.* 215:375–389.

Greenblatt, R. E., Y. Blatt, and M. Montal. 1985. The structure of the voltage sensitive sodium channel—inferences derived from computer-aided analysis of *Electrophorus electricus* primary structure. *FEBS Lett.* 193:125–134.

Guy, H. R. and Seetharamulu, P. 1986. Molecular model of the action potential sodium channel. *Proc. Natl. Acad. Sci. USA.* 83:508–512.

Hahin, R., and L. Goldman. 1978. Initial conditions and the kinetics of the sodium conductance in *Myxicola* giant axons. *J. Gen. Physiol.* 72:863–877.

Hanck, D. A., M. F. Sheets, and H. A. Fozzard. 1989. Immobilization of Na channel gating charge in single canine cardiac purkinje cells. *Biophys. J. 55:317a.* (Abstr.)

Heggeness, S. T., and J. G. Starkus. 1986. Saxitoxin and Tetrodotoxin. Electrostatic effects on sodium channel gating current in crayfish giant axons. *Biophys. J.* 49:629–643.

Hodgkin, A. L., and A. F. Huxley. 1952*a*. The dual effect of membrane potential on sodium conductance in the giant axon of *Loligo. J. Physiol. (Lond.).* 116:497–506.

Hodgkin, A. L., and A. F. Huxley, 1952*b*. A quantitative description of membrane current and its application to conduction and excitation in nerve. *J. Physiol. (Lond.)*. 117:500–544.

Huang, J. M., J. Tanguy, and J. Z. Yeh. 1987. Removal of sodium inactivation and block of sodium channels by chloramine-T in crayfish and squid giant axons. *Biophys. J.* 52:155–163.

Keynes, R. D. 1983. Voltage-gated ion channels in the nerve membrane. *Proc. R. Soc. Lond. B.* 220:1–30.

Keynes, R. D. 1986. Properties of the sodium gating current in the squid axon. *In* Tetrodotoxin, Saxitoxin and the Molecular Biology of the Sodium Channel. C. Y. Kao and S. R. Levinson, editors. *Ann. NY Acad. Sci.* 479:431–438.

Keynes, R. D. 1990. A series-parallel model of the voltage-gated sodium channel. *Proc. R. Soc. Lond.* 240:425–432.

Keynes, R. D., and E. Rojas. 1976. The temporal and steady-state relationships between activation of the sodium conductance and movement of the gating particles in the squid giant axon. *J. Physiol. (Lond.)*. 255:157–189.

Keynes, R. D., N. G. Greeff, and I. C. Forster. 1990. Kinetic analysis of the sodium gating current in the squid giant axon. *Proc. R. Soc. Lond. B.* 243:411–423.

Montal, M. 1990. Channel protein engineering: an approach to the identification of molecular determinants of function in voltage-gated and ligand-regulated channel proteins. *In* Ion Channels. T. Narahashi, editor. Plenum Press, New York. 2:1–32.

Noda, M., S. Shimizu, T. Tanabe, T. Takai, T. Kayano, T. Ikeda, H. Takahashi, H. Nakayama, Y. Kanaoka, N. Minamino, K. Kangawa, H. Matsuo, M. A. Raftery, T. Hirose, S. Inayama, H. Hayashida, T. Miyata, and S. Numa. 1984. Primary structure of *Electrophorus electricus* sodium channel deduced from cDNA sequence. *Nature (Lond.)*. 312:121–127.

Nonner, W. 1980. Relations between the inactivation of sodium channels and the immobilization of gating charge in frog myelinated nerve. *J. Physiol. (Lond.)*. 299:573–603.

Numa, S., and M. Noda. 1986. Molecular structure of sodium channels. *Ann. NY Acad. Sci.* 479:338–355.

Oxford, G. S. 1981. Some kinetic and steady-state properties of sodium channels after removal of inactivation. *J. Gen. Physiol.* 77:1–22.

Rayner, M. D., and J. G. Starkus. 1989. The steady state distribution of gating charge in crayfish giant axons. *Biophys. J.* 55:1–19.

Rayner, M. D., and J. G. Starkus. 1991. Kinetic fractionation of gating currents. *Biophys. J.* 59:71*a*. (Abstr.)

Ruben, P. C., J. G. Starkus, and M. D. Rayner. 1990. Holding potential affects the apparent voltage-sensitivity of sodium channel activation in crayfish giant axons. *Biophys. J.* 58:1169–1181.

Schauf, C. L., and J. O. Bullock. 1979. Modification of sodium channel gating in *Myxicola* giant axons by deuterium oxide, temperature, and internal cations. *Biophys. J.* 27:193–208.

Schauf, C. L., and J. O. Bullock. 1980. Solvent substitution as a probe of channel gating in *Myxicola*. Differential effects of D_2O on some components of membrane conductance. *Biophys. J.* 30:295–306.

Schauf, C. L., and J. O. Bullock. 1982. Solvent substitution as a probe of channel gating in *Myxicola*. Effects of D_2O on kinetic properties of drugs that occlude channels. *Biophys. J.* 37:441–452.

Shrager, P. 1974. Ionic conductance changes in voltage clamped crayfish axons at low pH. *J. Gen. Physiol.* 64:666–690.

Starkus, J. G., B. D. Fellmeth, and M. D. Rayner. 1981. Gating currents in the intact crayfish giant axon. *Biophys. J.* 35:521–533.

Starkus, J. G., S. T. Heggeness, and M. D. Rayner. 1984. Kinetic analysis of sodium channel block by internal methylene blue in pronased crayfish giant axons. *Biophys. J.* 46:205–218.

Starkus, J. G., and M. D. Rayner. 1987. Immobilization and nonimmobilization components in gating charge in crayfish giant axon. 1987. *Biophys. J.* 51:434*a*. (Abstr.)

Stuhmer, W., F. Conti. H. Suzuki, X. Wang, M. Noda, N. Yahagi, H. Kubo, and S. Numa. 1989. Structural parts involved in activation and inactivation of the sodium channel. *Nature (Lond.)*. 339:597–603.

Stimers, J. R., F. Bezanilla, and R. E. Taylor. 1985. Sodium channel activation in the squid giant axon. Steady-state properties. *J. Gen. Physiol.* 85:65–82.

Stimers, J. R., F. Bezanilla, and R. E. Taylor. 1987. Sodium channel gating currents. Origin of the rising phase. *J. Gen. Physiol.* 89:521–540.

Swensen, R. P. 1980. Gating charge immobilization and sodium channel activation in internally perfused crayfish axons. *Nature (Lond.)*. 287:644–645.

Taylor, R. E., and F. Bezanilla. 1983. Sodium and gating current time shifts resulting from changes in initial conditions. *J. Gen. Physiol.* 81:773–784.

Wang, G. K., M. S. Brodwick, and D. C. Eaton. 1985. Removal of sodium channel inactivation in squid axon by the oxidant chloramine-T. *J. Gen. Physiol.* 86:289–302.

Zagotta, W. N., and R. W. Aldrich. 1990. Voltage-dependent gating of Shaker A-type potassium channels in *Drosophila* muscle. *J. Gen. Physiol.* 95:29–60.

Zimmerberg, J., F. Bezanilla, and V. A. Parsegian. 1990. Solute inaccessible aqueous volume changes during opening of the potassium channel of the squid giant axon. *Biophys. J.* 57:1049–1064.